J. Membrane Biol. 208, 203–212 (2005)
DOI: 10.1007/s00232-005-7001-0

The Journal of
Membrane
Biology

The Glycine Residues G551 and G1349 within the ATP-Binding Cassette Signature Motifs Play Critical Roles in the Activation and Inhibition of Cystic Fibrosis Transmembrane Conductance Regulator Channels by Phloxine B

Patricia Melin*, Caroline Norez*, Isabelle Callebaut†, Frédéric Becq*

*Institut de Physiologie et Biologie Cellulaires, CNRS UMR6187, Université de Poitiers, 40 avenue du recteur Pineau, 86022 Poitiers, France

†Département de biologie structurale, IMPMC, CNRS UMR7590, Université Paris 6 et 7, case 115, 4 place Jussieu, 75252 Paris cedex 05, France

Received: 2 September 2005/Revised: 5 December 2005

Abstract. The cystic fibrosis transmembrane conductance regulator (CFTR) protein contains a canonical ATP-binding cassette (ABC) signature motif, LSGGQ, in nucleotide binding domain 1 (NBD1) and a degenerate LSHGH in NBD2. Here, we studied the contribution of the conserved residues G551 and G1349 to the pharmacological modulation of CFTR chloride channels by phloxine B using iodide efflux and whole-cell patch clamp experiments performed on the following green fluorescent protein (GFP)-tagged CFTR: wild-type, delF508, G551D, G1349D, and G551D/G1349D double mutant. We found that phloxine B stimulates and inhibits channel activity of wild-type CFTR (K_s = 3.2 ± 1.6 μM, K_i = 38 ± 1.4 μM) and delF508 CFTR (K_s = 3 ± 1.8 μM, K_i = 33 ± 1 μM). However, CFTR channels with the LSGDQ mutated motif (mutation G551D) are activated (K_s = 2 ± 1.13 μM) but not inhibited by phloxine B. Conversely, CFTR channels with the LSHDH mutated motif (mutation G1349D) are inhibited (K_i = 40 ± 1.01 μM) but not activated by phloxine B. Finally, the double mutant G551D/G1349D CFTR failed to respond not only to phloxine B stimulation but also to phloxine B inhibition, confirming the importance of both amino acid locations. Similar results were obtained with genistein, and kinetic parameters were determined to compare the pharmacological effects of both agents. These data show that G551 and G1349 control the inhibition and activation of CFTR by these agents, suggesting functional nonequivalence of the signature motifs of NBD in the ABC transporter CFTR.

Correspondence to: F. Becq; email: frederic.becq@univ-poitiers.fr

Key words: Cystic fibrosis — CFTR — ABC signature — G551D — G1349D — Phloxine B — Genistein — Non-Michaelis-Menten

Introduction

The cystic fibrosis (CF) transmembrane conductance regulator (CFTR) chloride channel belongs to the ATP-binding cassette (ABC) transporters, a large evolutionarily conserved family of integral membrane proteins that catalyze the active transport of a variety of solutes across biological membranes coupled to hydrolysis of nucleotides as a source of energy (Riordan et al., 1989; Vankeerberghen, Cuppens & Cassima, 2002). CFTR belongs to subfamily C and is coded ABCC7 in the ABC classification (http://nutrigene.4T.com/humanabc.htm). CFTR protein is composed of two repeated units joined by a long sequence called the regulatory (R) domain, the phosphorylation of which regulates channel activity (Tabcharani et al., 1991; Gadsby & Nairn, 1999; Ostedgaard, Baldursson & Welsh 2001). Each part has a membrane-spanning domain, including six transmembrane α-helices and a globular domain, the nucleotide binding domain (NBD), containing an adenosine triphosphate (ATP)-binding site. NBD contains highly conserved Walker A and B motifs in common with a variety of ATP-binding proteins (Walker et al., 1982; Gadsby & Nairn, 1999). The LSGGQ motif (also named *ABC signature sequence*) is located in the primary structure between the two Walker A and B motifs and shows remarkable conservation in NBDs of all ABC transporters except for CFTR, in which the signature sequences, although symmetrical, are not

equivalent – i.e., LSGGQ in NBD1 and LSHGH in NBD2 (Walker et al., 1982) – and except the transporter associated with antigen processing (TAP), containing a canonical LSGGQ motif in TAP1 but a degenerate LAAGQ motif in TAP2 (Chen, Abele & Tampe, 2004).

The fluorescein derivative phloxine B (PhlxB) has been used as a probe for various ATPases (Skou & Esmann, 1981; Mitchinson et al., 1982; Muallem & Karlish, 1983; Farley & Faller, 1985) and as a blocker of the activity of pancreatic K_{ATP} channels (de Weille, Muller & Lazdunski, 1992; Dickinson et al., 1997; Loffler-Walz & Quast, 1998). Due to structural and pharmacological analogies between CFTR and K_{ATP}, PhlxB has also been evaluated on the Cl^- current associated with the expression of human CFTR in *Xenopus* oocytes (Bachmann et al., 2000). Results showed a bell-shaped concentration dependence with midpoints at 45 and 1600 nM for the stimulatory and inhibitory phases, respectively (Bachmann et al., 2000). Then, similar effects with delF508 CFTR expressed in C127 mouse mammary epithelial cells have been shown (Cai & Sheppard, 2002), leading to the hypothesis that the drug could stimulate CFTR by interaction with the ATP-binding site of NBD2 to slow the dissociation of ATP from NBD1. A bell-shaped response is referred to as *non-Michaelis-Menten behavior*, a mechanism described for the effect of the isoflavone genistein on CFTR and for many enzymes and receptors (Derand, Bulteau-Pignoux & Becq, 2002; Melin et al., 2004). Such a mechanism could be explained in terms of the resulting interaction of stimulatory and inhibitory components involving two binding sites, one being the activator and the other being the inhibitor (Rovati & Nicosia, 1994; Bronnikov et al., 1999; Derand et al., 2002; Atkins, 2005).

The goal of this study was to investigate the contribution of the two conserved glycine residues G551 (LSGGQ) and G1349 (LSHGH) of the ABC signature motifs to the modulation of CFTR Cl^- channels by PhlxB. By comparing the pharmacological behavior of various constructs, our study highlighted their role in the control of inhibition (G551) and activation (G1349) of CFTR by PhlxB.

Materials and Methods

Construction of CFTR Mutants and Transfection

The pEGFP-C1-CFTR mammalian expression vector, allowing fusion of green fluorescent protein (GFP) to the N terminus of CFTR, was generously provided by K. H. Karlson (Dartmouth College, Hanover, NH). Individual delF508, G551D and G1349D mutations were created by site-directed mutagenesis as previously described (Melin et al., 2004). Double mutant G551D/G1349D (named 2GD-CFTR) was derived from pEGFP-G551D-CFTR. COS-7 cells were transfected 12–24 h after seeding, using cationic lipids (JetPEI™; Qbiogene, Illkirch, France) with 1 μg/ml of plasmid for iodide efflux experiments or 0.5 μg/ml for the patch-clamp method. The medium was refreshed 24 h posttransfection. COS-7 cells were cultured as described (Melin et al., 2004) and used 72 h after transfection for iodide efflux experiments and 24–48 h for electrophysiological measurements. Cells expressing CFTR proteins were visually identified in the patch-clamp setup by green fluorescence emission detected by the CKX41 culture microscope, supplied by the Olympus (Tokyo, Japan) Reflected Fluorescence System.

Electrophysiology

Ionic currents were measured in the broken-patch, whole-cell configuration of the patch-clamp method using an EPC-7 amplifier (List Electronic, Darmstadt, Germany). The holding potential was −40 mV in all whole-cell experiments. Current/voltage (I-V) relationships were built by clamping the membrane potential to −40 mV and by pulses from −100 to +100 mV in 20-mV increments. Pipettes were prepared by pulling borosilicate glass capillary tubes (GCL150-TF10; Clark Electromedical, Reading, UK) using a two-step vertical puller (Narishige, Tokyo, Japan). They were connected to the head stage of the patch-clamp amplifier through an Ag-AgCl pellet (pipette resistance of 3–5 MΩ). Pipette capacitance was electronically compensated in cell-attached mode. Membrane capacitance and series resistances were measured in the whole-cell mode by fitting capacitance currents, obtained in response to a hyperpolarization of 10 mV, with a first-order exponential, and by integrating the surface of the capacitance current. Voltage-clamp signals, allowing the membrane potential to be held at different values, were recorded via a microcomputer equipped with an analog/digital-digital/analog conversion board (Digidata 1200 interface; Axon Instruments, Burlingame, CA). Results were analyzed with pCLAMP version 6.03 software (Axon Instruments). The external bath solution contained (in mM) 145 NaCl, 4 CsCl, 1 $CaCl_2$, 1 $MgCl_2$, 10 glucose and 10 tetradecyl sulfate (TES) titrated with NaOH to pH 7. The osmolarity was 315 ± 5 mOsmol. The intrapipette solution contained (in mM) 113 L-aspartic acid, 113 CsOH, 27 CsCl, 1 NaCl, 1 $MgCl_2$, 1 ethyleneglycoltetraacetic acid, 3 MgATP (ex temporane) and 10 TES (titrated with CsOH to pH 7.2). The osmolarity was 285 ± 5 mOsmol. The pipette solution was always hypotonic (with respect to the bath solution) to prevent cell swelling and activation of the volume-sensitive chloride channels. All experiments were conducted at room temperature (20–25°C). The calculated chemical equilibrium potential for chloride (E_{Cl^-}) is −42 mV. All currents traces shown in the figures are single traces.

Radiotracer Efflux Experiments

Chloride channel activity was assayed by measuring the rate of iodide (^{125}I) efflux from a population of transfected COS-7 cells 72 h posttransfection, as previously described (Derand et al., 2002; Melin et al., 2004). Briefly, the fraction of initial intracellular ^{125}I lost during each time point was determined and time-dependent rates (k, min^{-1}) of ^{125}I efflux were calculated according to $k = \ln(^{125}I_{t1}/^{125}I_{t2})/(t_1 - t_2)$, where $^{125}I_t$ is the intracellular ^{125}I at time t and t_1 and t_2 are successive time points. Concentration-dependent activation curves were constructed by plotting k vs. time. To compare different sets of data from separate experiments, we calculated the relative rates $r = k_{peak} - k_{basal}$ (min^{-1}). In all experiments, the peak rate (k_{peak}) corresponds to the maximum value of the rate of efflux whereas the basal rate (k_{basal}) represents the third point on the graphs. For concentration-dependent inhibition curves, data were normalized using the relative rate without inhibitor as 100%. The non-Michaelian parameters K_s and K_i were determined as described (Derand et al., 2002). The half-maximal

effective inhibitory concentrations (IC_{50}) were estimated after fitting results by a nonlinear regression.

Chemicals

Forskolin and genistein were from LC Laboratories (PKC Pharmaceuticals, Woburn, MA). All other products were from Sigma (St. Louis, MO). Stock solutions were prepared at 30 and 100 mM in dimethyl sulfoxide (Me_2SO) for genistein and PhlxB, respectively. Dilution of stock solution allowed preparation of fresh solution at the final concentrations indicated in the text. The vehicle for drugs (final Me_2SO concentration 0.1%) has no effect on either basal iodide efflux, even at 1% (Melin et al., 2004), or currents.

Statistics

Results are expressed as mean ± standard error of the mean (SEM) of n observations. Data were compared with Student's t-test. Differences were considered statistically significant at $P < 0.05$. All statistical tests were performed using GraphPad Prism version 4.0 for Windows (GraphPad Software, San Diego, CA). Dose-response curves were compared posttest following two-way analysis of variance applying the Bonferroni correction.

Results

Properties of G1349D-CFTR Chloride Current

Individual delF508, G551D and G1349D and double G551D/G1349D (named *2GD-CFTR*) mutations were created by site-directed mutagenesis and inserted into the pEGFP-C1-CFTR mammalian expression vector, allowing fusion of GFP to the N terminus of CFTR as previously described (Melin et al., 2004). Figure 1 indicates the location of the LSGGQ and LSHGH domains in NBD1 and NBD2 (Fig. 1*A*), together with the location of G551 and G1349 within these sites (Fig. 1*B*). Transient transfection in COS-7 cells was performed, and the CFTR chloride channel activity was analyzed by patch-clamp recordings and iodide efflux. The basal whole-cell current (mean current density of 14 ± 4 pA/pF at +40 mV, $n = 3$) was not significantly affected by the expression of G1349D-CFTR (mean current density of 12 ± 3 pA/pF at +40 mV, $n = 7$; Fig. 2*A* and *D*). The class III mutation G1349D, like G551D, impaired activation of CFTR channels by the adenylate cyclase activator forskolin (Fsk). The corresponding mean current densities are 11 ± 4 pA/pF for G551D-CFTR and 9 ± 4 pA/pF for G1349D-CFTR at +40 mV in the presence of 10 μM Fsk ($n = 3$). Using iodide efflux experiments, we tested increasing concentrations of Fsk from 0.1 to 100 μM but failed to stimulate any iodide efflux in G1349D-CFTR-expressing cells ($n = 4$ for each concentration, not shown). However, these class III mutant CFTR channels are activatable by a cocktail composed of 10 μM Fsk and 100 μM of the phosphodiesterase inhibitor 3-isobutyl-1-methylxanthine (IBMX) (Melin et al., 2004; Becq & Mettey, 2005). The presence of Fsk/IBMX in the extracellular bath activated a current (mean current density of 88 ± 13 pA/pF at +40 mV, $n = 4$; Fig. 2*B*) that reversed at –40 mV (Fig. 2*D*), a value close to the theoretical Cl^- equilibrium potential imposed in our conditions ($E_{Cl^-} = -42$ mV), confirming its Cl^- nature. The cyclic adenosine monophosphate (cAMP)-activated G1349D-CFTR Cl^- current was completely inhibited by 100 μM glibenclamide (Fig. 2*C* and *D*) (Sheppard & Welsh, 1993). Using iodide efflux experiments, we determined the concentration dependence of the effect of glibenclamide on G1349D-CFTR and G551D/G1349D (noted *2GD*) in cells activated by 10 μM Fsk + 100 μM IBMX. We calculated IC_{50} values of 8.3 ± 1.06 μM for G1349D-CFTR ($n = 4$; black symbols, Fig. 2*E*) and 5.5 ± 1.13 μM for 2GD-CFTR ($n = 4$; open symbols, Fig. 2*E*). Differences between the two curves were not statistically significant ($P < 0.05$) using analysis of variance followed by a Bonferroni post hoc test.

Non-Michaelian Modulation by PhlxB of Wild-Type- and delF508-CFTR Channels

The fluorescein derivative PhlxB has been described as an allosteric blocker of wild-type (wt)-CFTR Cl^- channels (Bachmann et al., 2000; Cai & Sheppard, 2002). We explored the effect of PhlxB on the Cl^- channel activity of the following CFTR mutants: delF508, G551D, G1349D and 2GD. We first compared the pharmacological behavior of wt- and delF508-CFTR in the presence of the drug. To overcome the processing defect of delF508 mutation and promote its delivery to the cell membrane, COS-7 cells transfected with delF508-CFTR were cultured for 24 h at 27°C (Denning et al., 1992; Melin et al., 2004). Figure 3A presents the iodide efflux measured in response to increasing concentrations of PhlxB in the presence of 0.5 μM Fsk for wt-CFTR- and delF508-CFTR-expressing cells. Fsk was used in all experiments because PhlxB alone is inefficient on nonphosphorylated CFTR Cl^- channels expressed in COS-7 cells (*data not shown*) or other cells (Cai & Sheppard, 2002). We obtained bell-shaped concentration-response curves (Fig. 3A), typical of non-Michaelis-Menten behavior, as described earlier for the isoflavone genistein (Derand et al., 2002; Melin et al., 2004). For concentrations of 1–10 μM, we found marked stimulation of wt- and delF508-CFTR channel activity (Fig. 3A). For concentrations of 10–100 μM PhlxB, the chloride channel activity of CFTR was inhibited (Fig. 3A). Table 1 presents the corresponding kinetic parameters for activation (K_s) and inhibition (K_i) by PhlxB of wt-CFTR and delF508-CFTR. Importantly, the K_s and K_i values calculated for wt-CFTR are not significantly affected by the delF508 mutation of CFTR. However, with delF508-CFTR-expressing cells, the overall magnitude of the

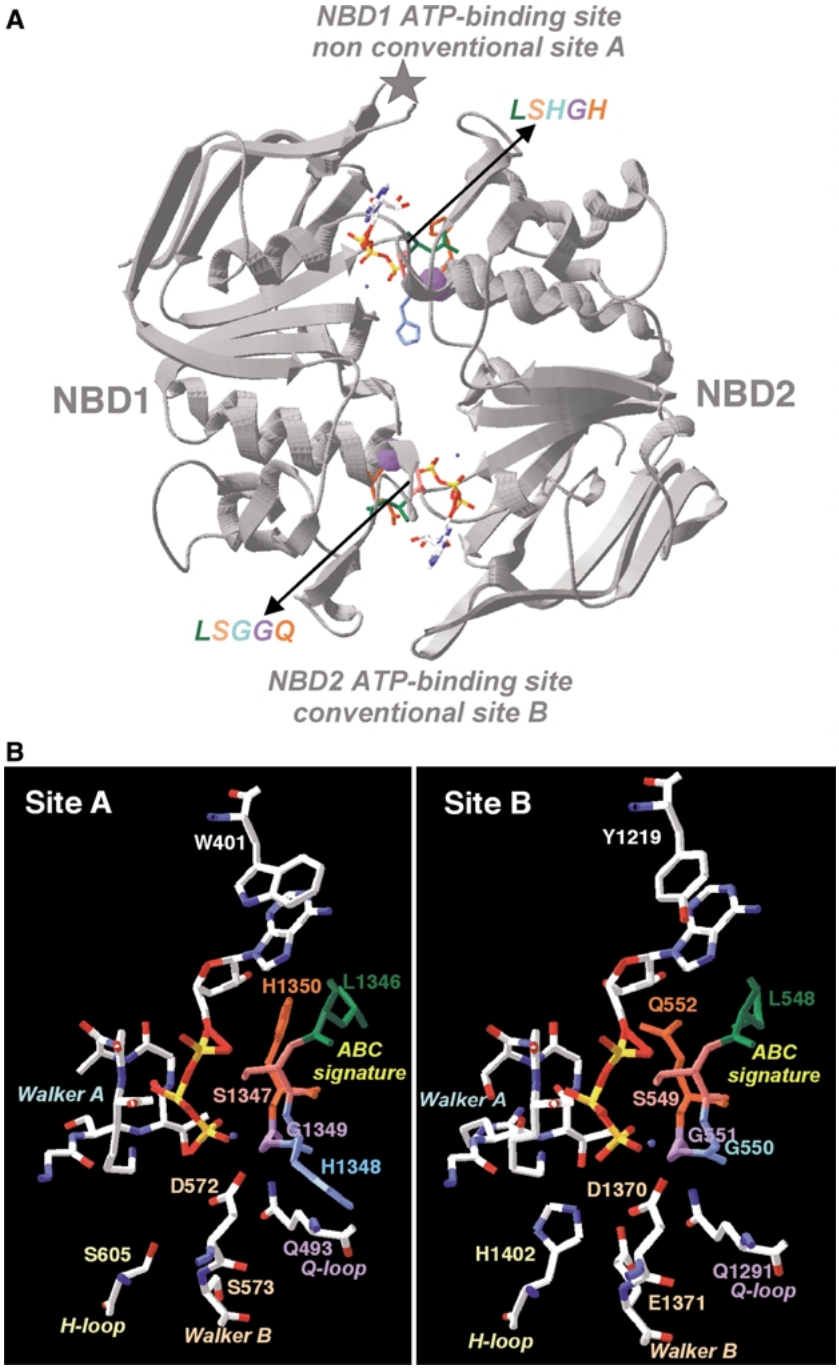

Fig. 1. Location of G551 and G1349 in the LSGGQ/LSHGH motifs of CFTR. (*A*) Ribbon representation of the model of the CFTR NBD1/NBD2 head-to-tail heterodimer (Callebaut et al., 2004; Eudes et al., 2005). The ABC signatures (LSGGQ and LSHGH) are shown in atomic details together with the ATP molecules. (*B*) Detailed view of the two ATP-binding sites, which were superimposed. Amino acids from the different conserved motifs are shown.

response to PhlxB is smaller compared to that of wt-CFTR (Fig. 3A), as previously shown for genistein (Melin et al., 2004). These results confirm the existence of two opposite effects of PhlxB on wt- and delF508-CFTR activities, i.e., stimulation at low concentrations and inhibition at high concentrations.

Effects of PhlxB on G551D, G1349D and G551D/G1349D Channels

In the next series of experiments, we examined the consequence of the glycine-to-aspartic acid mutations in NBD1 and NBD2 on the response to PhlxB in the presence of Fsk. A classical sigmoidal concentration-response relationship describes the effect of PhlxB on G551D (Fig. 3B, black triangles). These results indicate a complete loss of inhibition at high PhlxB concentrations (>10 μM) of G551D-CFTR compared to wt-CFTR (*see* Fig. 3*A*). The calculated $K_s = 2 \pm 1.13$ μM ($n = 4$) shows that PhlxB is a potent activator of G551D channels (Table 1). Then, we examined the response to PhlxB of G1349D channels also in the presence of Fsk. Contrary to the previous results with the NBD1 mutation G551D, we

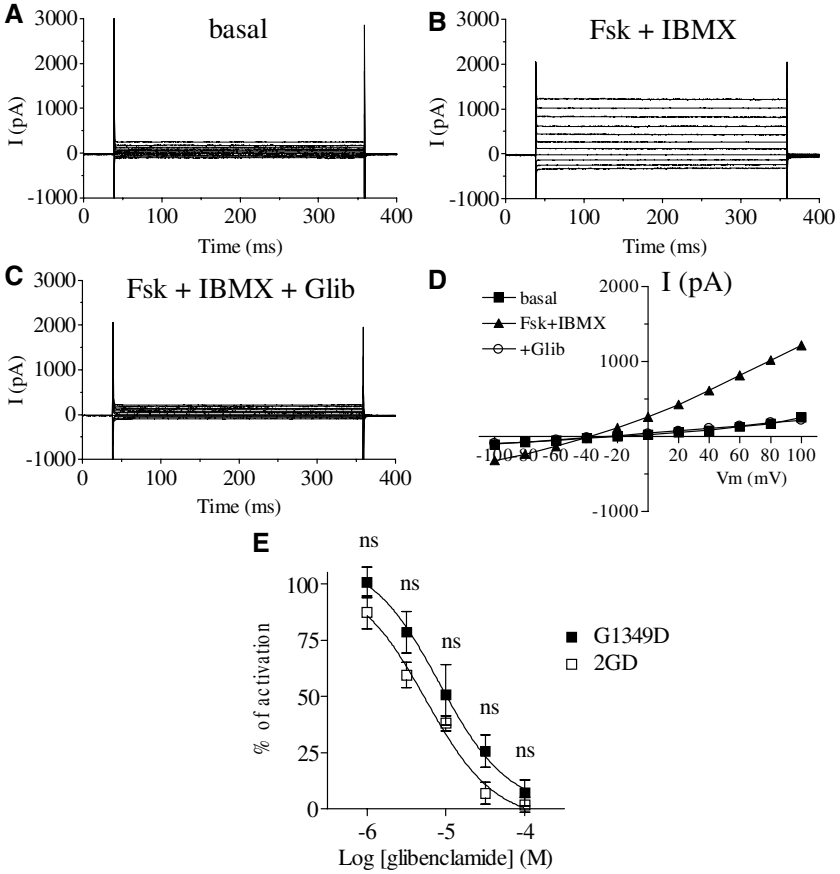

Fig. 2. Activation by cAMP cocktail and inhibition by glibenclamide of G1349D-CFTR channels. Representative whole-cell current traces for CFTR are shown before (*A*) and after (*B*) application of cAMP cocktail (Fsk 10 μM + IBMX 100 μM) and following application of 100 μM glibenclamide (Glib, *C*). (D) Step protocol consisted of 400 ms voltage steps from −100 to +100 mV from a holding potential of −40 mV. Capacitance of the cell is 15 pF. Vm, membrane voltage; (*E*) Concentration-responses curves of glibenclamide on COS-7 cells transfected with GFP-G1349D-CFTR and 2GD after maximal activation with cAMP cocktail. Data are presented as mean ± SEM, $n = 4$, for each concentration. The relative rate is calculated as described in Materials and Methods and normalized to the relative rate with cAMP cocktail, without glibenclamide. IC_{50} values calculated in these conditions are for G1349D channels, 8.3 ± 1.06 μM, and for 2GD channels, 5.55 ± 1.13 μM. ns, nonsignificant.

found no evidence for stimulation of G1349D channels by increasing concentrations of PhlxB despite the presence of Fsk (Fig. 3B, black squares). The double mutant, carrying G551D and G1349D mutations, is also refractory to PhlxB stimulation (Fig. 3*B*, open squares). These data show, first, that mutation of glycine 551 in NBD1 abolished the inhibition, but not the activation, of CFTR by PhlxB and, second, that mutation of glycine 1349 in NBD2 (single or double CFTR mutant) abolished the activation of CFTR by PhlxB.

Effect of PhlxB when G1349D-, G551D- and 2GD-CFTR-Expressing Cells are Stimulated by Fsk/IBMX

Because the mutant G1349D can be activated by Fsk/IBMX but not by Fsk/PhlxB, we took advantage of this difference to investigate whether PhlxB could nevertheless inhibit the mutant channel after its activation by Fsk/IBMX, like the wt-CFTR channels. In the following experiments, we performed whole-cell patch-clamp experiments on COS-7 cells expressing G1349D-CFTR stimulated by Fsk/IBMX and subsequently challenged by application of 10 μM PhlxB into the bath. A representative time course of the amplitude of the current density is illustrated Fig. 4*A*. The current amplitude (pA) measured between +40 and −40 mV (*see* insert Fig. 4*A*) was plotted as a function of time and normalized by cell capacitance (pF) to allow comparison between cell densities (pA/pF). Addition of 10 μM Fsk + 100 μM IBMX in the bath medium induced a significant increase of Cl^- current (Fig. 4*A* and *B*). After stable activation of the G1349D-CFTR current, addition of 10 μM PhlxB (in the continuous presence of Fsk/IBMX) inhibited G1349D-CFTR currents (Fig. 4*A* and *B*). In approximately 2 min, the current returned to the basal level. Further application of 100 μM glibenclamide in the extracellular bath had no additional inhibitory effect (Fig. 4*A*), confirming that the G1349D-CFTR current was totally inhibited by PhlxB. Averaged values and statistical analysis for the different experimental protocols described are given (Fig. 4*C* and *D*).

Then, similar experiments were performed with G551D-CFTR-expressing cells. As expected from iodide efflux experiments, a significant increase of Cl^- current was recorded in G551D-expressing cells stimulated by 10 μM Fsk + 100 μM IBMX (Fig. 5*A* and *B*). However, contrary to G1349D-CFTR, PhlxB did not inhibit G551D-CFTR currents after stable activation of G551D (compare left and right whole-cell

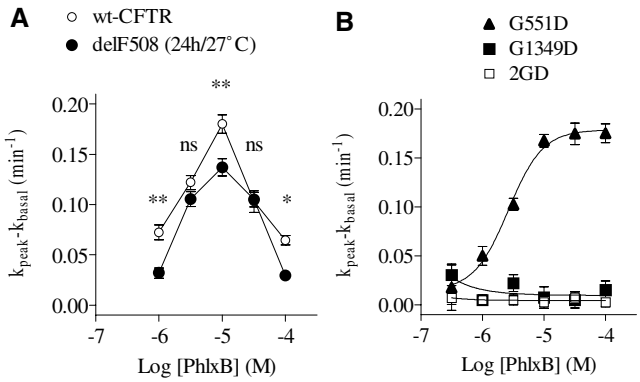

Fig. 3. Effect of PhlxB on wt-CFTR chloride channels and CF-associated mutants. (*A*) Concentration-response curves of PhlxB on COS-7 cells transiently transfected with GFP-wt-CFTR and delF508 (after cell exposure at 27°C for 24 h) in the presence of 0.5 μM Fsk. The relationships are bell-shaped, with an inflection point at 10 μM of PhlxB. Note that the amplitude of delF508-CFTR activity channels is less important than for wt-CFTR. (*B*) Concentration-response curves of PhlxB on COS-7 cells transiently transfected with GFP-CFTR with the following mutations: G551D, -G1349D and -2GD. Note that 10 μM Fsk is required for these mutants. ns, nonsignificant; $*P < 0.05$, $**P < 0.01$.

Table 1. Kinetic parameters for activation (K_s) and inhibition (K_i) of CFTR by PhlxB and genistein[a]

	PhlxB		Genistein	
Construct	K_s	K_i	K_s	K_i
wt-CFTR	3.2 ± 1.6	38 ± 1.4	10 ± 1[b]	106 ± 1[b]
delF508	3 ± 1.8	33 ± 1	9.8 ± 1[b]	107 ± 1[b]
G551D	2 ± 1.13	–[d]	13 ± 1.25[b]	–
G1349D	–	40 ± 1.01[c]	–	121 ± 1.14[c]
2GD	–	–	–	–

[a] All data (in μM) are $n = 4$.
[b] Data from Melin et al., 2004.
[c] With activation by Fsk/IBMX.
[d] No effect.

traces, Fig. 5*B*). PhlxB did not potentiate G551D-CFTR currents due to maximal stimulation of the current by Fsk/IBMX (Fig. 5*A* and *C*). Further application of 100 μM glibenclamide in the extracellular bath fully inhibited the currents (Fig. 5*A* and *C*), confirming that G551D-CFTR is refractory to inhibition only by PhlxB but not by glibenclamide. Averaged values and statistical analysis for the different experimental protocols described above are given (Fig. 5*C* and *D*). We also noted two differences between G551D and G1349D-CFTR channels stimulated by Fsk + IBMX. First, the time to maximal current stimulation with G551D-CFTR, 120 ± 9 s ($n = 4$), was significantly faster ($P < 0.01$) than that for G1349D (194 ± 8 s, $n = 4$). Second, the current density measured at +40 mV was 26 ± 5 pA/pF ($n = 6$) for G551D construct, a value approximately threefold smaller ($P < 0.001$) than the current density measured for G1349D, 88 ± 13 pA/pF ($n = 4$).

Finally, we determined the concentration-dependent inhibitory effects of PhlxB and genistein on G1349D and 2GD-CFTR channels after stimulation by Fsk/IBMX (Fig. 6). CFTR activity was normalized (as percent of maximal activation) with respect to the relative rate prior to addition of PhlxB or genistein. We calculated the K_i for PhlxB on G1349D (40 ± 1.01 μM, $n = 4$ for each concentration; Fig. 6A, black symbols). For 2GD-CFTR channels, no inhibition occurred; the calculated relative rates in the presence or absence of PhlxB or genistein were not statistically different (Fig. 6A and B, open symbols). With genistein, the calculated K_i was 121 ± 1.14 μM for G1349D channels ($n = 4$ for each concentration; Fig. 6B, black symbols). Table 1 gives all the kinetic parameters determined in this study.

Discussion

In the present study, we investigated the pharmacological properties of wt-CFTR and CFTR mutated in the ABC signature domains of both NBD1 and NBD2 expressed in COS-7 cells challenged by PhlxB. At low concentrations, the fluorescein derivative PhlxB stimulates wt- and delF508-CFTR but also inhibits both channels at higher concentrations. With the LSGGQ motif mutated at the G551 location (i.e., LSGDQ), CFTR can be activated but not inhibited by PhlxB or genistein. With the LSHGH motif mutated at G1349 (i.e., LSHDH), CFTR channel activity can be inhibited but not stimulated by PhlxB or genistein. The combination of two aspartic substitutions has additive effects; i.e., with both mutated glycine residues (i.e., LSGDQ/LSHDH), PhlxB, like Gst, is unable to activate and inhibit CFTR channel activity, demonstrating nonequivalent and complementary roles for each single glycine. Thus, interaction of the pharmacological agents PhlxB and genistein with glycine G551 in LSGGQ triggers inhibition of CFTR channel activity and with glycine G1349 in the LSHGH motif allows channel activation.

The elucidation of the three-dimensional structures of several NBDs from various ABC transporters, including NBD1 of CFTR, has revealed their specific architecture and, for some, their organization into functional homo- or heterodimers into a "head-to-tail" configuration (Schmitt & Tampe, 2002; Callebaut et al., 2004; Lewis et al., 2004). In this configuration, each nucleotide is sandwiched between the two NBDs and each nucleotide-binding site is formed by the Walker A, Walker B, Q-loop and

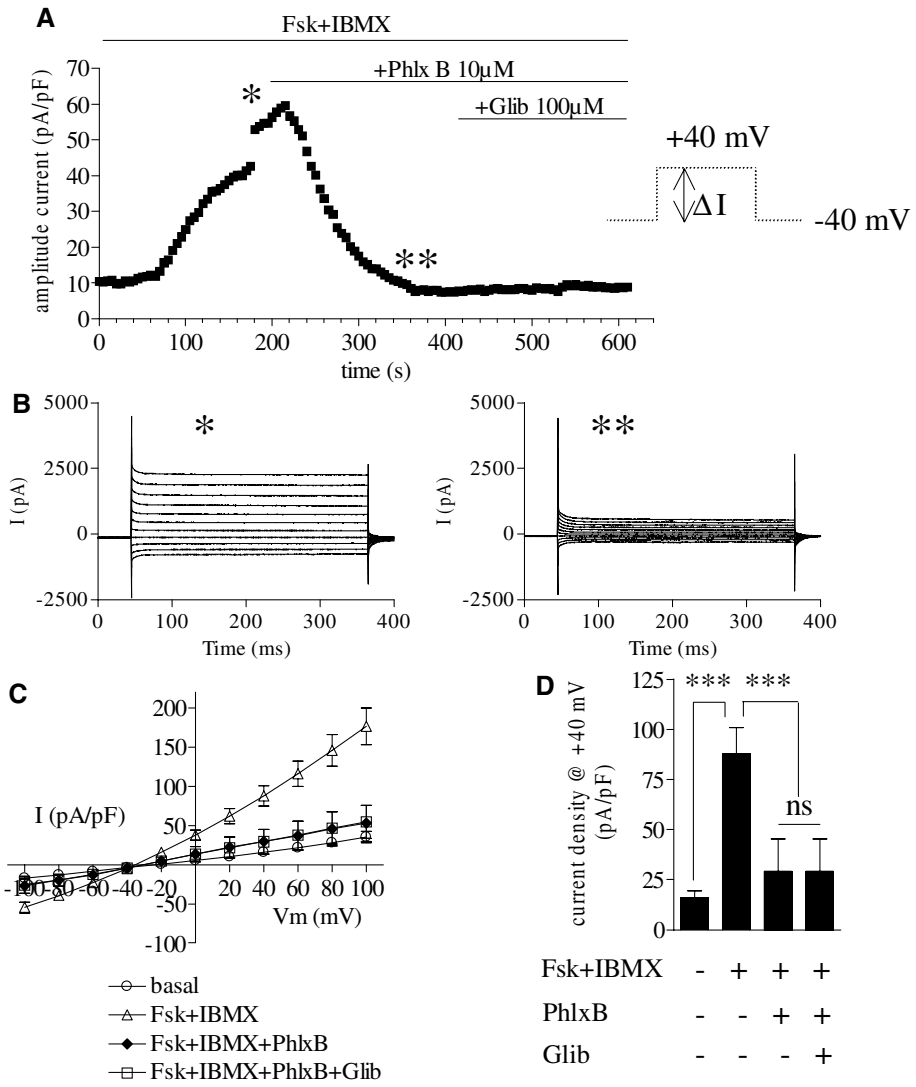

Fig. 4. Effects of PhlxB on cAMP-stimulated G1349D-CFTR channels. (*A*) Representative time course of G1349D-CFTR current amplitude in the presence of various agonists. (*B*) Representative trace of current recorded on G1349D channels with Fsk + IBMX (*) and with Fsk + IBMX + PhlxB (**). (*C*) I/V relationships for G1349D-CFTR chloride current (mean ± SEM) normalized by cell capacitance. Cells were held at −40 mV and clamped with 400 ms voltage pulses from −100 to +100 mV. Vm, membrane voltage. (*D*) Summary of current amplitudes (mean ± SEM between +40 and −40 mV) recorded on cells transfected with GFP-CFTR-G1349D in various conditions: basal ($n = 4$), Fsk + IBMX ($n = 4$), Fsk + IBMX + PhlxB ($n = 4$), Fsk + IBMX + PhlxB + glibenclamide (Glib, $n = 4$). ns, nonsignificant; $***P < 0.001$.

switch of one NBD and the signature sequence of the other NBD. The CFTR NBD1/NBD2 heterodimer structure has been modeled (Callebaut et al., 2004; Eudes et al., 2005) based on the head-to-tail architecture which has also been shown for CFTR to produce optimal catalytic activity (Kidd et al., 2004). An asymmetry of the two ATP-binding sites is observed in the CFTR NBD1/NBD2 heterodimer, as shown in Figure 1, with highly degenerated sequences of the different motifs surrounding the noncanonical ATP-binding site. This asymmetry is supported by experimental data (Aleksandrov et al., 2002; Basso et al., 2003; Berger, Ikuma & Welsh, 2005) showing that rapid ATP turnover occurs at a canonical site (named *site B* or *NBD2 ATP-binding site* as it is formed by the Walker A and Walker B motifs of NBD2 and the nonmodified signature sequence LSGGQ of NBD1), whereas ATP remains bound for a long time, in a nonhydrolyzed form, at a noncanonical site (*named site A* or *NBD1 ATP-binding site*, in which participate the Walker A and Walker B motifs of NBD1 and the highly modified signature sequence LSHGH of NBD2).

These observations are consistent with a general model for the channel-gating mechanism, in which channel opening and closing are driven by ATP binding and hydrolysis at the NBD2 ATP-binding site (conventional site B, Fig. 1), respectively, whereas binding and (weak) hydrolysis at the NBD1 ATP-binding site (nonconventional site A, Fig. 1) is only a prerequisite for channel opening (Gunderson & Kopito, 1995). Interestingly our data show that G1349D-CFTR elicited a larger Cl^- current than G551D-CFTR, these two glycine residues being located within the NBD1 and NBD2 active sites, respectively (Fig. 1*B*). These results are indeed in agreement with recent studies that propose that CFTR channel opening and closing occur predominantly at NBD2 (Aleksandrov et al., 2002; Basso et al., 2003; Berger et al., 2005). In the current head-to-tail model of CFTR organization, the active site for ATPase activity involves Walker A and B of one

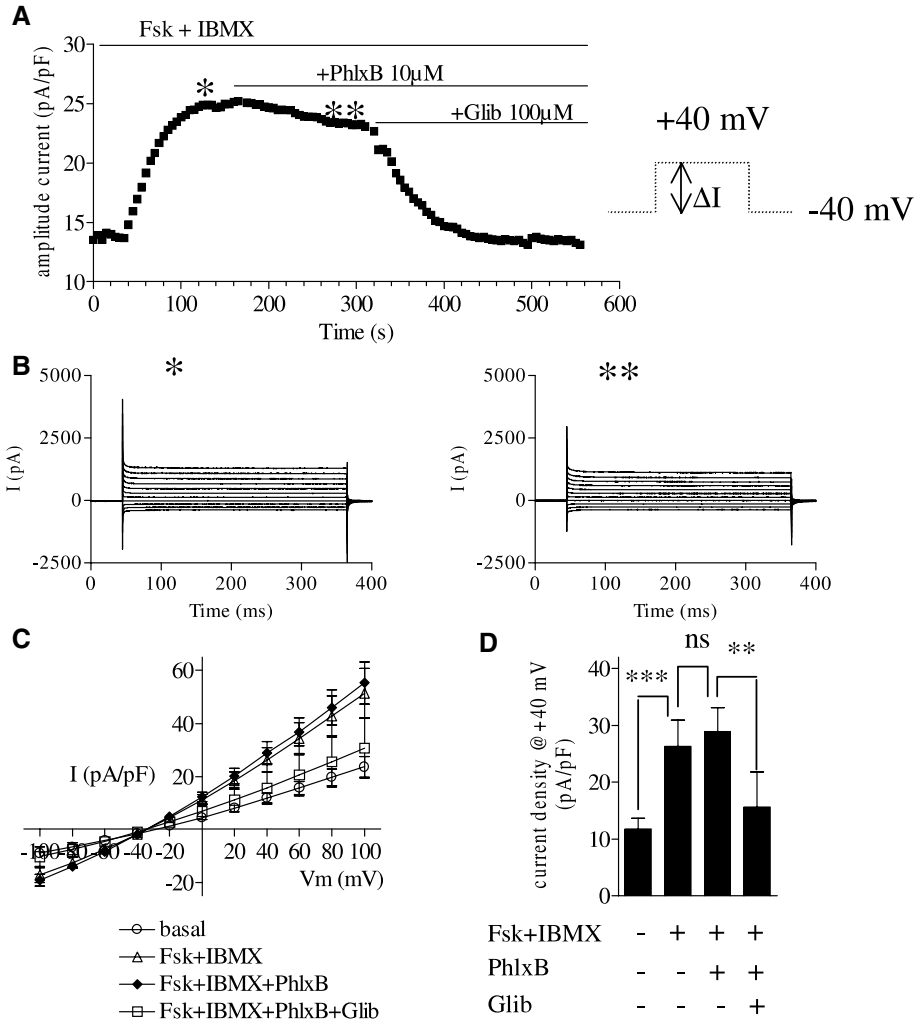

Fig. 5. Effects of PhlxB on cAMP-activated G551D-CFTR channels. (*A*) Representative time course of G551D-CFTR amplitude current in the presence of various agonists. (*B*) Representative trace of current recorded on G551D channels with Fsk + IBMX (*) and with Fsk + IBMX + PhlxB (**). (*C*) I/V relationships for the G551D-CFTR channels (mean ± SEM) normalized by cell capacitance. (*D*) Summary of current amplitudes (mean ± SEM between +40 and −40 mV) recorded on cells transfected with GFP-G551D-CFTR in various conditions: basal (n = 10), Fsk + IBMX (n = 6), Fsk + IBMX + PhlxB (n = 5), Fsk + IBMX + PhlxB + glibenclamide (Glib, n = 3). ns,nonsignificant; $^{**}P < 0.01$, $^{***}P < 0.001$.

NBD plus the signature sequence of the opposite NBD. Therefore, for ATPase activity of NBD2, the LSGGQ sequence of NBD1 is required. According to these data, we show that the LSGDQ mutated sequence (with G551D) drastically impairs activation of CFTR Cl^- channel activity by Fsk/IBMX compared to the LSHDH mutated sequence (with G1349D). The asymmetrical nature of the NBD heterodimer further supports such a model.

Several reports have suggested that CFTR activators use different mechanisms. Drugs like genistein and PhlxB are associated with direct binding at the NBDs (Randak et al., 1999; Cai & Sheppard, 2002), consistent with our observations that CFTR modulation is altered by NBD mutations G551D and G1349D. The pharmacological effects of other drugs like benzoquinolizinium and IBMX are not altered by these mutations (Melin et al., 2004), suggesting on the contrary an effect, or binding if any, at a distance from NBDs. For most of the activators, the molecular mechanisms of their pharmacological effects remain unknown (Becq & Mettey, 2005). On the other hand, it was expected that all CFTR channels studied here would be inhibited by glibenclamide since recent studies identified glibenclamide binding sites located outside NBDs (Sheppard & Robinson, 1997; Linsdell, 2005). The existence of multiple sites was proposed to explain the effect of PhlxB on CFTR (Bachmann et al., 2000; Cai & Sheppard, 2002), with one site to stimulate CFTR located in NBD2 (which we now propose to be G1349). Using single patch-clamp recordings, Cai and Sheppard (2002) identified one possible inhibitory site that would be only 4% of the way through the transmembrane electric field from the inside. However, these authors favored another interpretation by suggesting that PhlxB might block the channel pore by binding to one, two, or more sites. In support of that, PhlxB has two negative charges located on different parts of the molecule. Therefore, G551 may be one of these sites, another being located close to or within the pore. However, using *Xenopus* oocytes expressing wt-CFTR, Bachmann et al. (2000) concluded that PhlxB inhibited CFTR currents by interfering with channel gating rather than by blocking the channel pore from the inside. Therefore, although we clearly identified two

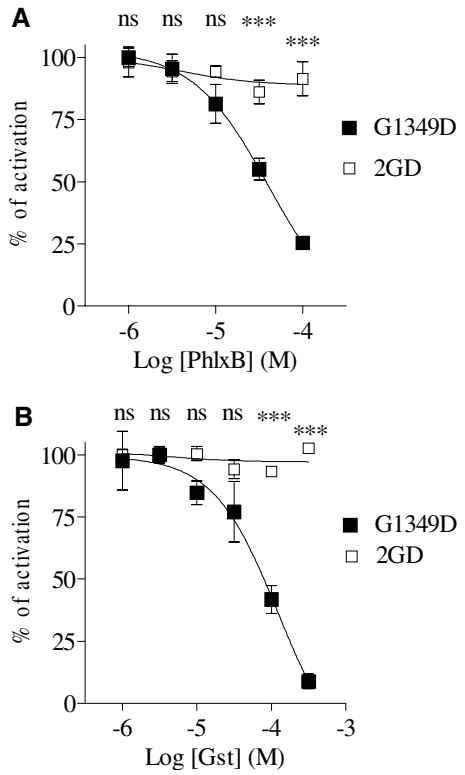

Fig. 6. Comparison of inhibitory effect of PhlxB and genistein on cAMP-activated G1349D- and 2GD-CFTR channels. Concentration-response curves of PhlxB (*A*) and genistein (*B*). Data are expressed as percentage of maximal activation with Fsk + IBMX. ns, nonsignificant; ***$P < 0.001$

important sites for activation and inhibition of CFTR by PhlxB, we certainly cannot exclude the possibility that multiple inhibitory sites exist.

Based on molecular docking simulations (Moran, Galietta & Zegarra-Moran, 2005), some potential binding sites for CFTR activators were predicted in the interface of the NBD dimer. The most probable one strongly involves the participation of the NBD1 active site (nonconventional site A), in which G1349 is included, and, to a lesser extent, the NBD2 active site (conventional site B), including G551. A possible mechanism suggested for the mechanism of CFTR activators is stabilization of the heterodimer upon binding of the drug to its site in the NBD interface, resulting in an increase at the activity periods (Moran et al., 2005). The effect of the mutations studied here on the stimulatory and inhibitory effects of genistein and PhlxB suggest that the corresponding amino acids in wt-CFTR are directly involved in the drug active sites. This hypothesis is therefore in agreement with the proposal of drug binding site(s) located at the interface of NBDs (Moran et al., 2005). The activation site may directly involve the NBD1 ATP-binding site as the amino acid G1349 appeared, as shown by our study, to control the activation of CFTR. This site may correspond to the site 2 described by Moran et al. (2005) as this one principally involves amino acids of the NBD1 ATP-binding site. Regarding this hypothesis, the drug would principally acts as a stabilization factor of the heterodimer interface, preventing its dissociation upon hydrolysis of ATP. The inhibitor site would have an opposite effect, thus promoting the heterodimer dissociation. This site may directly involve the conventional NBD2 ATP-binding site as the amino acid G551 was clearly shown in this study to control this inhibition.

In conclusion, although further studies will be required to probe evidence of binding sites with these agents, our data identified the conserved glycine residues of the signature sequences of CFTR as molecular determinants for activation (G1349) and inhibition (G551) of CFTR by two chemically unrelated agents, phloxine B and genistein. These results highlighted the important role of ABC signature motifs in the pharmacological regulation of CFTR chloride channel activity.

We thank Dr. V. Thoreau, Dr. F. Bilan, Dr. K. H. Karlson and Dr. B. A. Stanton for the pS65T/EGFP-C1/WT-CFTR construct; Marlène Baudis for the delF508-CFTR construct; and N. Bizard for assistance with cell cultures. This work was performed as part of the thesis of P. M. at Ingénierie chimique, Biologique et Géologique (ICBG) thesis school at Poitiers University, supported by a thesis fellowship from the Region Poitou-Charentes. This work was also supported by specific grants from CF-Pronet and Vaincre La Mucoviscidose and an institutional grant from the CNRS and Région Poitou-Charentes.

References

Aleksandrov, L., Aleksandrov, A.A., Chang, X.B., Riordan, J.R. 2002. The first nucleotide binding domain of cystic fibrosis transmembrane conductance regulator is a site of stable nucleotide interaction, whereas the second is a site of rapid turnover. *J. Biol. Chem.* **277:**15419–15425

Atkins, W.M. 2005. Non-Michaelis-Menten kinetics in cytochrome P450-catalyzed reactions. *Annu. Rev. Pharmacol. Toxicol.* **45:**291–310

Bachmann, A., Russ, U., Waldegger, S., Quast, U. 2000. Potent stimulation and inhibition of the CFTR Cl^- current by phloxine B. *Br. J. Pharmacol.* **131:**433–440

Basso, C., Vergani, P., Nairn, A.C., Gadsby, D.C. 2003. Prolonged nonhydrolytic interaction of nucleotide with CFTR's NH2-terminal nucleotide binding domain and its role in channel gating. *J. Gen. Physiol.* **122:**333–348

Becq, F., Mettey, Y. 2005. Pharmacological interventions for the correction of ion transport defect in cystic fibrosis. *Expert Opin. Ther. Targets* **14:**1465–1483

Berger, A.L., Ikuma, M., Welsh, M.J. 2005. Normal gating of CFTR requires ATP binding to both nucleotide-binding domains and hydrolysis at the second nucleotide-binding domain. *Proc. Natl. Acad. Sci. U.S.A.* **102:**455–460

Bronnikov, G.E., Zhang, S.J., Cannon, B., Nedergaard, J. 1999. A dual component analysis explains the distinctive kinetics of cAMP accumulation in brown adipocytes. *J. Biol. Chem.* **274:**37770–37780

Cai, Z., Sheppard, D.N. 2002. Phloxine B interacts with the cystic fibrosis transmembrane conductance regulator at multiple sites to modulate channel activity. *J. Biol. Chem.* **277:**19546–19553

Callebaut, I., Eudes, R., Mornon, J.P., Lehn, P. 2004. Nucleotide-binding domains of human cystic fibrosis transmembrane conductance regulator: Detailed sequence analysis and three-dimensional modeling of the heterodimer. *Cell. Mol. Life Sci.* **61:**230–242

Chen, M., Abele, R., Tampe, R. 2004. Functional non-equivalence of ATP-binding cassette signature motifs in the transporter associated with antigen processing (TAP). *J. Biol. Chem.* **279:**46073–46081

Denning, G.M., Anderson, M.P., Amara, J.F., Marshall, J., Smith, A.E., Welsh, M.J. 1992. Processing of mutant cystic fibrosis transmembrane conductance regulator is temperature-sensitive. *Nature* **358:**761–764

Derand, R., Bulteau-Pignoux, L., Becq, F. 2002. The cystic fibrosis mutation G551D alters the non-Michaelis-Menten behavior of the cystic fibrosis transmembrane conductance regulator (CFTR) channel and abolishes the inhibitory genistein binding site. *J. Biol. Chem.* **277:**35999–36004

de Weille, J.R., Muller, M., Lazdunski, M. 1992. Activation and inhibition of ATP-sensitive K^+ channels by fluorescein derivatives. *J. Biol. Chem.* **267:**4557–4563

Dickinson, K.E., Bryson, C.C., Cohen, R.B., Rogers, L., Green, D.W., Atwal, K.S. 1997. Nucleotide regulation and characteristics of potassium channel opener binding to skeletal muscle membranes. *Mol. Pharmacol.* **52:**473–481

Eudes, R., Lehn, P., Ferec, C., Mornon, J.P., Callebaut, I. 2005. Nucleotide binding domains of human CFTR: A structural classification of critical residues and disease-causing mutations. *Cell. Mol. Life Sci.* **62:**2112–2123

Farley, R.A., Faller, L.D. 1985. The amino acid sequence of an active site peptide from the H,K-ATPase of gastric mucosa. *J. Biol. Chem.* **260:**3899–3901

Gadsby, D.C., Nairn, A.C. 1999. Regulation of CFTR Cl^- ion channels by phosphorylation and dephosphorylation. *Adv. Second Messenger Phosphoprotein Res.* **33:**79–106

Gunderson, K.L., Kopito, R.R. 1995. Conformational states of CFTR associated with channel gating: The role ATP binding and hydrolysis. *Cell* **82:**231–239

Kidd, J.F., Ramjeesingh, M., Stratford, F., Huan, L.J., Bear, C.E. 2004. A heteromeric complex of the two nucleotide binding domains of cystic fibrosis transmembrane conductance regulator (CFTR) mediates ATPase activity. *J. Biol. Chem.* **279:** 41664–41669

Lewis, H.A., Buchanan, S.G., Burley, S.K., Conners, K., Dickey, M., Dorwart, M., Fowler, R., Gao, X., Guggino, W.B., Hendrickson, W.A., Hunt, J.F., Kearins, M.C., Lorimer, D., Maloney, P.C., Post, K.W., Rajashankar, K.R., Rutter, M.E., Sauder, J.M., Shriver, S., Thibodeau, P.H., Thomas, P.J., Zhang, M., Zhao, X., Emtage, S. 2004. Structure of nucleotide-binding domain 1 of the cystic fibrosis transmembrane conductance regulator. *EMBO J.* **23:**282–293

Linsdell, P. 2005. Location of a common inhibitor binding site in the cytoplasmic vestibule of the cystic fibrosis transmembrane conductance regulator chloride channel pore. *J. Biol. Chem.* **280:**8945–8950

Loffler-Walz, C., Quast, U. 1998. Binding of K(ATP) channel modulators in rat cardiac membranes. *Br. J. Pharmacol.* **123:**1395–1402

Melin, P., Thoreau, V., Norez, C., Bilan, F., Kitzis, A., Becq, F. 2004. The cystic fibrosis mutation G1349D within the signature motif LSHGH of NBD2 abolishes the activation of CFTR chloride channels by genistein. *Biochem. Pharmacol.* **67:**2187–2196

Mitchinson, C., Wilderspin, A.F., Trinnaman, B.J., Green, N.M. 1982. Identification of a labelled peptide after stoicheiometric reaction of fluorescein isothiocyanate with the Ca^{2+}-dependent adenosine triphosphatase of sarcoplasmic reticulum. *FEBS Lett.* **146:**87–92

Moran, O., Galietta, L.J., Zegarra-Moran, O. 2005. Binding site of activators of the cystic fibrosis transmembrane conductance regulator in the nucleotide binding domains. *Cell. Mol. Life Sci.* **62:**446–460

Muallem, S., Karlish, S.J. 1983. Catalytic and regulatory ATP-binding sites of the red cell Ca^{2+} pump studied by irreversible modification with fluorescein isothiocyanate. *J. Biol. Chem.* **258:**169–175

Ostedgaard, L.S., Baldursson, O., Welsh, M.J. 2001. Regulation of the cystic fibrosis transmembrane conductance regulator Cl^- channel by its R domain. *J. Biol. Chem.* **276:**7689–7692

Randak, C., Auerswald, E.A., Assfalg-Machleidt, I., Reenstra, W.W., Machleidt, W. 1999. Inhibition of ATPase, GTPase and adenylate kinase activities of the second nucleotide-binding fold of the cystic fibrosis transmembrane conductance regulator by genistein. *Biochem. J.* **340:**227–235

Riordan, J.R., Rommens, J.M., Kerem, B., Alon, N., Rozmahel, R., Grzelczak, Z., Zielenski, J., Lok, S., Plavsic, N., Chou, J.L., Drumm, M.L, Ianozzi, C., Collins, F.S., Tsui, L.C. 1989. Identification of the cystic fibrosis gene: Cloning and characterization of complementary DNA. *Science* **245:**1066–1073

Rovati, G.E., Nicosia, S. 1994. Lower efficacy: Interaction with an inhibitory receptor or partial agonism? *Trends Pharmacol. Sci.* **15:**140–144

Schmitt, L., Tampe, R. 2002. Structure and mechanism of ABC transporters. *Curr. Opin. Struct. Biol.* **12:**754–760

Sheppard, D.N., Robinson, K.A. 1997. Mechanism of glibenclamide inhibition of cystic fibrosis transmembrane conductance regulator Cl^- channels expressed in a murine cell line. *J. Physiol.* **503:**333–346

Sheppard, D.N., Welsh, M.J. 1993. Inhibition of the cystic fibrosis transmembrane conductance regulator by ATP-sensitive K^+ channel regulators. *Ann. N.Y. Acad. Sci.* **707:**275–284

Skou, J.C., Esmann, M. 1981. Eosin, a fluorescent probe of ATP binding to the (Na^+ + K^+)-ATPase. *Biochim. Biophys. Acta* **647:**232–240

Tabcharani, J.A., Chang, X.B., Riordan, J.R., Hanrahan, J.W. 1991. Phosphorylation-regulated Cl^- channel in CHO cells stably expressing the cystic fibrosis gene. *Nature* **352:**628–631

Vankeerberghen, A., Cuppens, H., Cassiman, J.J. 2002. The cystic fibrosis transmembrane conductance regulator: an intriguing protein with pleiotropic functions. *J. Cyst. Fibros.* **1:**13–29

Walker, J.E., Saraste, M., Runswick, M.J., Gay, N.J. 1982. Distantly related sequences in the alpha- and beta-subunits of ATP synthase, myosin, kinases and other ATP-requiring enzymes and a common nucleotide binding fold. *EMBO J.* **1:** 945–951